

Circuit Models for Conducted Susceptibility Analyses of Multiconductor Shielded Cables

Saih Mohamed, Rouijaa Hicham, Ghammaz Abdelilah

Abstract—This paper presents circuit models to analyze the conducted susceptibility of multiconductor shielded cables in frequency domains using Branin's method, which is referred to as the method of characteristics. These models, which can be used directly in the time and frequency domains, take into account the presence of both the transfer impedance and admittance. The conducted susceptibility is studied by using an injection current on the cable shield as the source. Two examples are studied; a coaxial shielded cable and shielded cables with two parallel wires (i.e., twinax cables). This shield has an asymmetry (one slot on the side). Results obtained by these models are in good agreement with those obtained by other methods.

Keywords—Circuit models, multiconductor shielded cables, Branin's method, coaxial shielded cable, twinax cables.

I. INTRODUCTION

SHIELDED cables are usually used in wired communication systems to protect signal transmission from external electromagnetic interference (EMI). Nevertheless, the cable shield may collect the electromagnetic disturbances produced by external fields generating EMI in the apparatus. It is therefore highly important for Electromagnetic Compatibility (EMC) studies to develop software tools capable of predicting induced effects in shielded cables configurations.

The prediction of these disturbances, which are usually induced by external fields or lumped sources, is a classical issue which can be dealt with in a variety of ways. Hence, it can be treated in the frequency domain, and therefore the induced responses of shielded cables are solved by using multiconductor transmission line (MTL) theory [1]-[3].

During the last years, a lot of researches have been set on the development of simulation program with integrated circuit emphasis (SPICE) equivalent circuit models for multi conductor transmission lines without shields excited by an incident electromagnetic field [4], [5], but the work on SPICE equivalent circuits for shielded cables began later than that on multi conductor transmission lines without shields. Caniggia and Maradei proposed some SPICE models to analyze the conducted immunity of both lossless and lossy coaxial cables

[6]. These models can be used for the frequency-domain analysis and the inverse Fourier transform (IFT) is needed to get the transient results.

Some SPICE models were proposed to analyze bulk current injection test on lossless shielded cables in the time and frequency domains [7], [8], where the injection clamp was considered as a longitudinal lumped current source. These models were employed to study the effects of the shield's grounding, geometrical and electrical asymmetries, and the cable's length on the terminal voltages presented in [9];

The main reason of this paper is to study the conducted susceptibilities of multi conductor shielded cables in frequency domain using the method of characteristics (Branin's method) [10]. This shield has an asymmetry (one slot on the side). The model works in frequency and time domain with linear and non linear loads, respectively; this allows it to be easily inserted in circuit simulators, such as Spice, Sabar, and Esacap [11]. The method is validated by comparing results with other methods.

II. DEVELOPMENT OF CIRCUIT MODELS FOR MULTICONDUCTOR SHIELDED CABLES

A. MTL Model of Shielded Cables

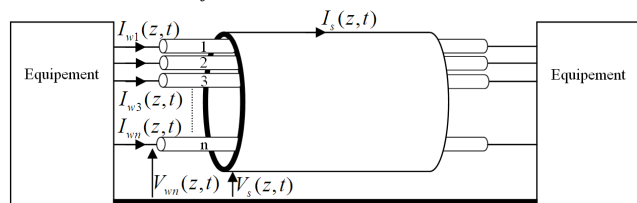


Fig. 1 Magnitude of the frequency responses in decibels of the inner

B. Terminations

The Telegrapher's equations for a multiconductor shielded cable with N parallel wires located inside the shield above the ground, as shown in Fig. 1, can be described by:

Outer system

$$\begin{cases} \frac{\partial V_s(z,t)}{\partial z} + L_s \frac{\partial I_s(z,t)}{\partial t} + R_s I_s(z,t) = 0 \\ \frac{\partial I_s(z,t)}{\partial z} + C_s \frac{\partial V_s(z,t)}{\partial t} + G_s V_s(z,t) = 0 \end{cases} \quad (1)$$

Saih Mohamed (corresponding author) and Ghammaz Abdelilah are with Laboratory of Electrical Systems and Telecommunications, Department of Physics, Faculty of Sciences and Technology, Cadi Ayyad University, Marrakesh, Morocco (e-mail: saih.mohamed2@gmail.com, aghammaz@yahoo.fr).

Rouijaa Hicham is with Laboratory of Electrical Systems and Telecommunications, Department of Applied Physics, Faculty of Sciences and Technology, Hassan First University, Settat, Morocco (e-mail: hruijaa@hotmail.com).

Inner system

$$\begin{cases} \frac{\partial V_w(z,t)}{\partial z} + L_w \frac{\partial I_w(z,t)}{\partial t} + R_w I_w(z,t) = Z_t I_s(z,t) \\ \frac{\partial I_w(z,t)}{\partial z} + C_w \frac{\partial V_w(z,t)}{\partial t} + G_w V_w(z,t) = 0 \end{cases} \quad (2)$$

where V_s is the shield-to-ground voltage, I_s is the current flowing between the external shield and the ground, $V_w = [V_{w1}, V_{w2}, \dots, V_{wN}]^T$ is the inner voltage vector whose k th element V_{wk} is the voltage of the k th wire versus the internal part of the shield, and $I_w = [I_{w1}, I_{w2}, \dots, I_{wN}]^T$ is the inner current vector whose k th element I_{wk} is the current of the k th wire. L_s , C_s , R_s and G_s are the per-unit-length (p.u.l) inductance, capacitance, resistance and conductance of the outer system, respectively, while L_w , C_w , R_w and G_w are the p.u.l inductance, capacitance, resistance, and conductance matrices of the inner system. $Z_t = [Z_{t1}, Z_{t2}, \dots, Z_{tN}]^T$ is the transfer impedance vector whose k th element Z_{tk} is the shield transfer impedance relative to the k th wire, is given by

$$Z_t = R_t + j\omega L_t \quad (3)$$

where R_t is the constant p.u.l. transfer resistance of the shield, and L_t is the p.u.l. transfer inductance due to the penetration of the magnetic field through the braid's apertures.

In order to implement the model in a simple fashion, it is necessary to restrict the result to lossless lines, i.e., $R_w = G_w = R_s = G_s = 0$

C. Coupling Conducted Immunity

In the classical equations of transmission lines, we have partial differential equations coupled to each other via mutual capacitances and inductances system. The equivalent method with independent line represents these couplings by means of voltage and current sources so-called 'controlled sources' [12].

$$\begin{cases} V_w = T_V V_{wm} \\ I_w = T_I I_{wm} \end{cases} \quad (4)$$

Substituting (4) into (2) gives:

$$\begin{cases} \frac{d}{dz} V_{wm} + j\omega L_{wm} I_{wm} = T_V^{-1} Z_t I_s \\ \frac{d}{dz} I_{wm} + j\omega C_{wm} V_{wm} = 0 \end{cases} \quad (5)$$

where

$$L_{wm} = T_V^{-1} L_w T_I \quad (6)$$

$$C_{wm} = T_I^{-1} C_w T_V \quad (7)$$

with L_{wm} and C_{wm} , diagonal matrices of dimension $N \times N$. T_V and T_I are selected so that the matrices L_{wm} and C_{wm} are diagonals.

After calculating L_{wm} and C_{wm} matrices, we determine the characteristic impedance Z_{cmi} and T_i the delay associated with each conductor.

$$Z_{cmi} = \sqrt{\frac{L_{wm_{ij}}}{C_{wm_{ij}}}} \quad (8)$$

$$T_i = \ell \sqrt{L_{wm_{ij}} \cdot C_{wm_{ij}}} \quad i = j; i = 1 \dots N \quad (9)$$

where ℓ is the length of the cable. In order to solve (1) and (2) we use the 'discrete line' model. For this reason, the cable is discretized in the form of cell; the length of each cell is $\lambda/10$, as shown in Fig. 2.

The solution to (1) and (2) for each cell is as follows:

$$\begin{cases} V_s(z_0 + \Delta z) = \varphi_{s11}(\Delta z) V_s(z_0) + \varphi_{s12}(\Delta z) I_s(z_0) \\ I_s(z_0 + \Delta z) = \varphi_{s21}(\Delta z) V_s(z_0) + \varphi_{s22}(\Delta z) I_s(z_0) \end{cases} \quad (10)$$

$$\begin{cases} V_w(z_0 + \Delta z) = \varphi_{11}(\Delta z) V_w(z_0) + \varphi_{12}(\Delta z) I_w(z_0) \\ \quad + Z_t I_s(z_0 + \Delta z) \\ I_w(z_0 + \Delta z) = \varphi_{21}(\Delta z) V_w(z_0) + \varphi_{22}(\Delta z) I_w(z_0) \end{cases} \quad (11)$$

where $\varphi_{s11}(\Delta z)$, $\varphi_{s12}(\Delta z)$, $\varphi_{s21}(\Delta z)$ and $\varphi_{s22}(\Delta z)$ are the elements of chain parameter matrix given by,

$$\varphi_{s11}(\Delta z) = \varphi_{s22}(\Delta z) = \cos(\beta \Delta z) \quad (12)$$

$$\varphi_{s12}(\Delta z) = -j\omega \frac{\sin(\beta \Delta z)}{\beta} L_s \quad (13)$$

$$\varphi_{s21}(\Delta z) = -j\omega \frac{\sin(\beta \Delta z)}{\beta} C_s \quad (14)$$

Substituting (4) into (11), we obtain:

$$\begin{cases} V_{wm}(z_0 + \Delta z) = \varphi_{m11}(\Delta z) V_{wm}(z_0) + \varphi_{m12}(\Delta z) I_{wm}(z_0) \\ \quad + Z_t I_s(z_0 + \Delta z) \\ I_{wm}(z_0 + \Delta z) = \varphi_{m21}(\Delta z) V_{wm}(z_0) + \varphi_{m22}(\Delta z) I_{wm}(z_0) \end{cases} \quad (15)$$

where the modal chain-parameter submatrices become;

$$\varphi_{m11}(\Delta z) = \frac{1}{2} (e^{j\omega M \Delta z} + e^{-j\omega M \Delta z}) \quad (16)$$

$$\varphi_{m12}(\Delta z) = -\frac{1}{2} Z_{cm} (e^{j\omega M \Delta z} - e^{-j\omega M \Delta z}) \quad (17)$$

$$\varphi_{m21}(\Delta z) = -\frac{1}{2} Z_{cm}^{-1} (e^{j\omega M \Delta z} - e^{-j\omega M \Delta z}) \quad (18)$$

$$\varphi_{m22}(\Delta z) = \frac{1}{2} (e^{j\omega M \Delta z} + e^{-j\omega M \Delta z}) \quad (19)$$

$$M^2 = T_I^{-1} C_w L_w T_I \quad (20)$$

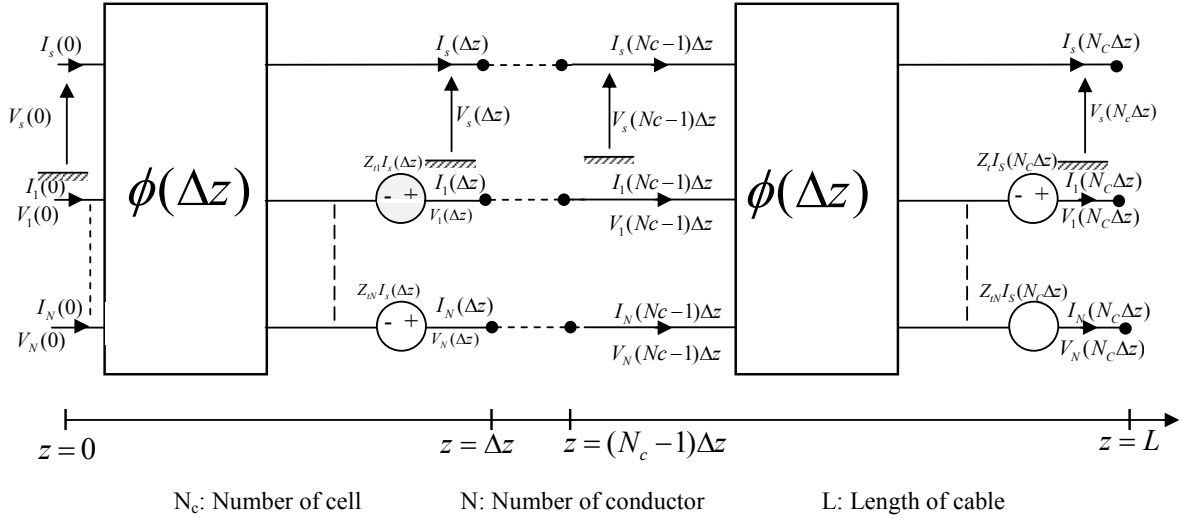


Fig. 2 Model of a Multiconductor shielded cables in the form of cells

D. Equivalent Circuit Model

After calculating the parameters of multiconductor lines, we move to the representation of a combination of shield /internal conductors using an equivalent circuit model.

Substituting (16), (17), (18), and (19) into (15), then (12), (13), and (14) into (10) gives:

$$\begin{cases} V_s(z_0) - Z_{cs} I_s(z_0) = e^{-j\omega T_s} [V_s(z_0 + \Delta z) - Z_{cs} I_s(z_0 + \Delta z)] \\ V_s(z_0 + \Delta z) + Z_{cs} I_s(z_0 + \Delta z) = e^{-j\omega T_s} [V_s(z_0) + Z_{cs} I_s(z_0)] \end{cases} \quad (21)$$

$$\begin{cases} V_{wm}(z_0) - Z_{cm} I_{wm}(z_0) = e^{-j\omega M \Delta z} [V_{wm}(z_0 + \Delta z) - Z_{cm} I_{wm}(z_0 + \Delta z) - T_V^{-1} Z_t I_s(z_0 + \Delta z)] \\ V_{wm}(z_0 + \Delta z) + Z_{cm} I_{wm}(z_0 + \Delta z) = e^{-j\omega M \Delta z} [V_{wm}(z_0) + Z_{cm} I_{wm}(z_0) + T_V^{-1} Z_t I_s(z_0 + \Delta z)] \end{cases} \quad (22)$$

Here T_s is the one-way delay of the outer system and is defined as $T_s = \Delta z \sqrt{C_s L_s}$. Z_{cs} is the characteristic impedance of the outer system and is defined as $Z_{cs} = \sqrt{L_s / C_s}$. The terms of the 'controlled' generators of voltage and current placed in each conductor of the cell are:

$$[V(z, t)]_i = \sum_{k=1}^N \{ [T_V]_{ik} [V_{wm}(z, t)]_k \} \quad (23)$$

$$[I_{wm}(z, t)]_i = \sum_{k=1}^N \{ [T_I^{-1}]_{ik} [I(z, t)]_k \} \quad (24)$$

III. SIMULATION RESULTS AND VALIDATION

A. Conducted Susceptibility Analysis of Coaxial Cable

The analysis of the conducted immunity is carried out on the coaxial cable over a ground plane. The length L and the

height h of the cable are 300m and 1cm, respectively. The shield radius is $r_s=2.5$ mm, the inner wire radius is $r_w=0.25$ mm, the internal dielectric constant is $\epsilon_r=1.77$. The values of the transfer resistance and inductance are: $R_T=10$ mΩ/m and $L_T=1.3$ nH/m. The terminal loads between the shield and the ground are $R_{S1}=1$ MΩ and $R_{S2}=123$ Ω, while the inner terminations are matched $R_{w1}=100$ Ω and $R_{w2}=100$ Ω. The current source is $I=1$ A. As shown in Fig. 3.

The differential mode voltages in the frequency domain analysis are shown in Fig. 4. The results show that the solutions from different methods are in good agreement.

In Fig. 4, the coupling into end side load is clearly stronger than in near side load, because the injection is asymmetrically located on near side of external shield: the configuration is physically similar to the coupling into single wire over ground plane with an illumination E_x - K_z , travelling along the wire in $+z$ direction [3]. Because the internal line is well matched by both side terminations, the total coupling is under a flat envelop and the anti-resonance frequencies are located as by the following formula $F = n [3E8 / (\lambda / 2) \sqrt{\epsilon}]$, $n = 1, 3, 5, \dots$, i.e. resonance at $\lambda/2$ shifted down by the internal dielectric constant.

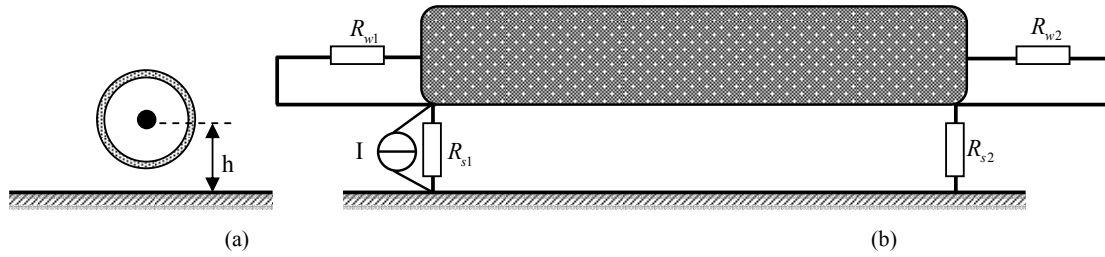


Fig. 3 (a) Geometrical cross-section of the coaxial cable (b) Configuration of the simulation for conducted analysis

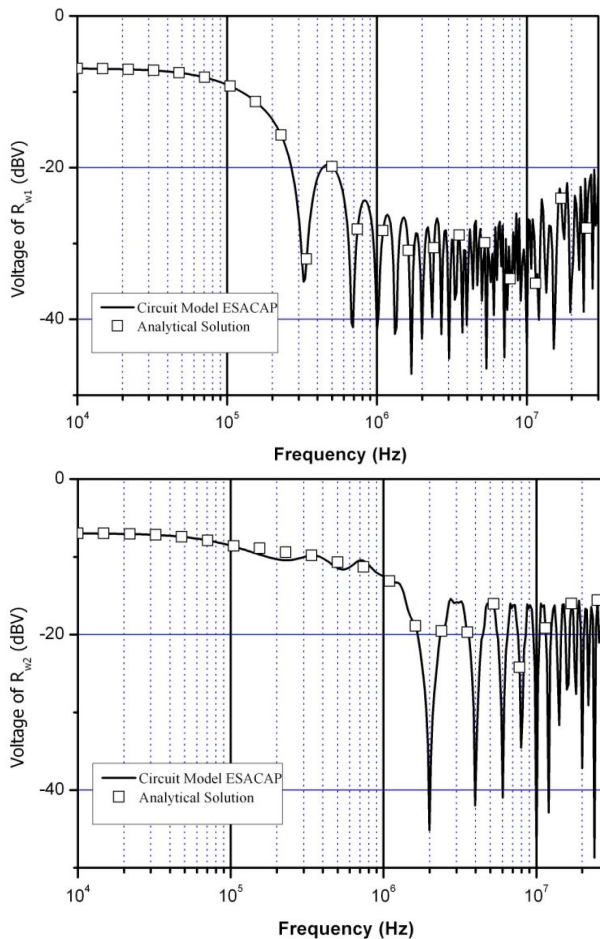


Fig. 4 Magnitude of the frequency responses in decibels of the inner terminations

B. Conducted Susceptibility Analysis of Twinax Shielded Cable

A twinax shielded cable over a ground plane is considered. The length is $L=300\text{m}$. The current source in parallel to near side pigtail of the shield is $I = 1\text{A}$. This shield has an asymmetry (one slot on the side) which is translated with the transfer parameters $L_{T1}=1.33\text{nH/m}$, $L_{T2}=1.2\text{nH/m}$ and $R=0$. The height above the ground plane is $h=1\text{cm}$. The wire radius $r_{w1}=r_{w2}=0.25\text{mm}$ and the distance from central axis of symmetry is $d1=d2=0.25\text{mm}$. As shown in Fig. 5, where the terminal loads between, the shield and ground are $R_1=1\text{M}\Omega$ and $R_2=124.7\Omega$. R_{w1} , R_{w2} and R_{w3} are 176Ω , 176Ω , and 61Ω , and the loads at the right termination has the same value as those at the left end.

The voltages induced on the differential loads at both ends of internal flat pair ($R_{w3}=61\Omega$) are calculated over the frequency range $F=10\text{KHz}-10\text{Mhz}$.

As shown in Fig. 6, the maximum value of differential coupling is located at far end of internal flat pair, for the same reason mentioned on the previous example “coax over ground plane”, i.e. the asymmetric position of input source. The coupled value is increasing with frequency at $+20\text{dB/dec}$ due to preponderant effect of transfer inductance, (the transfer resistance is zero).

The two curves show different values at frequency increase only because of unbalance of the two transfer inductance values.

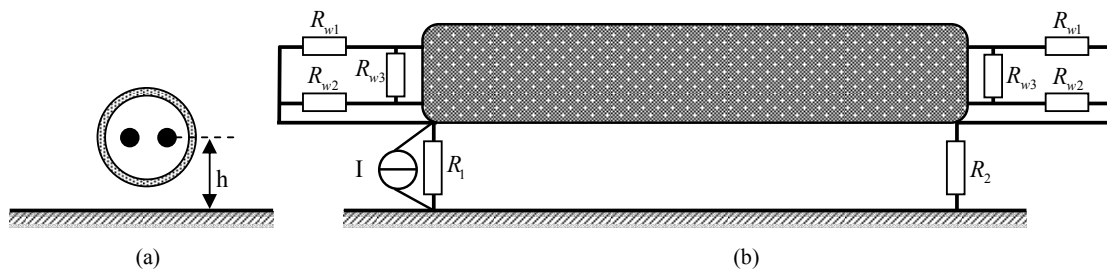


Fig. 5 (a) Geometrical cross-section of the Twinax cable. (b) Configuration of the simulation for conducted analysis

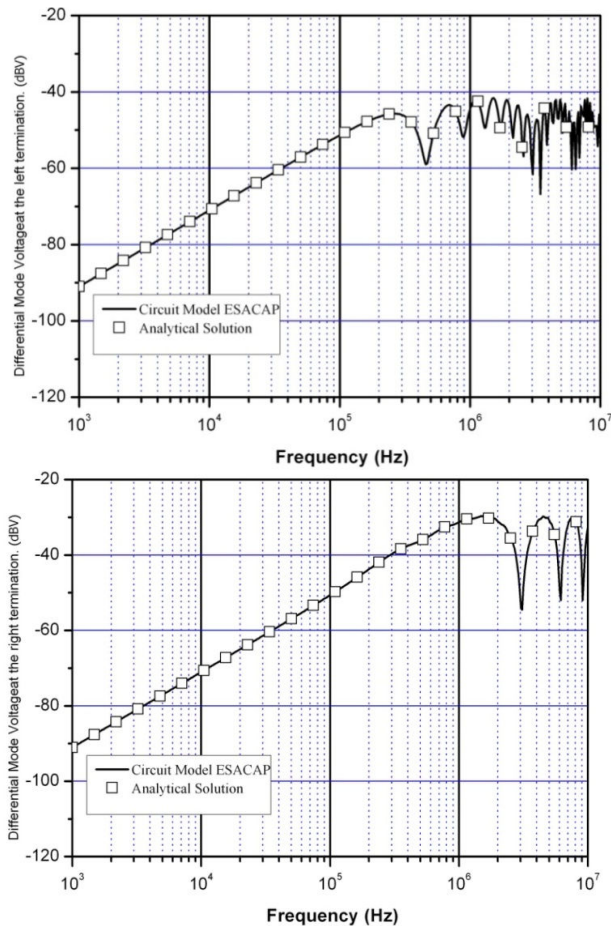


Fig. 6 Differential mode voltage induced on the twinax cable

IV. CONCLUSION

A circuit model for the analysis of the conducted susceptibility of multiconductor shielded cables has been developed and validations have been given in this paper. These models, which can be used directly in the time and frequency domains, take into account the presence of both the transfer impedance and admittance. Hence, they can be implemented to compute transient responses without the IFT. The results agree well with those obtained through other methods.

REFERENCES

- [1] Aguet, M.; Ianovici, M.; Lin, C.C.: Transient electromagnetic field coupling to long shielded cables, *IEEE Trans. Electromagn. Compat.*, 4, 1980, 276–282
- [2] M. D'Amore, M.; Feliziani, M.: Induced fast transients in multiconductor shielded cable, in *Proc. 7th Int. Conf. Electromagn. Compat.*, York, U.K., 1990, 103–108
- [3] Saih, M.; Rouijaa, H.; Ghammaz, A.: Coupling of electromagnetic waves with the RG58 cable, *International Conference on Multimedia Computing and Systems*, Marrakesh, Morocco, 2014.
- [4] C. R. Paul, "A SPICE model for multiconductor transmission lines excited by an incident electromagnetic field," *IEEE Trans. Electromagn. Compat.*, vol. 36, no. 4, pp. 342–354, Nov. 1994.
- [5] H. Xie, J. Wang, R. Fan, and Y. Liu, "A hybrid FDTD-SPICE method for transmission lines excited by a nonuniform incident wave," *IEEE Trans. Electromagn. Compat.*, vol. 51, no. 3, pp. 811–817, Aug. 2009.
- [6] S. Caniggia and F. Maradei, "Equivalent circuit models for the analysis of coaxial cables immunity," in *Proc. 2003 IEEE Int. Symp. Electromagn. Compat.*, vol. 2, pp. 881–886.
- [7] A. Orlandi, "Circuit model for bulk current injection test on shielded coaxial cables," *IEEE Trans. Electromagn. Compat.*, vol. 45, no. 4, pp. 602–615, Nov. 2003
- [8] G. Antonini and A. Orlandi, "Spice equivalent circuit of a two-parallelwires shielded cable for evaluation of the RF induced voltages at the terminations," *IEEE Trans. Electromagn. Compat.*, vol. 46, no. 2, pp. 189–198, May 2004.
- [9] G. Antonini, A. C. Scogna, and A. Orlandi, "Grounding, unbalancing and length effects on termination voltages of a twinax cable during bulk current injection," *IEEE Trans. Electromagn. Compat.*, vol. 46, no. 2, pp. 302–308, May 2004.
- [10] Branin Jr F. H.: Transient analysis of lossless transmission lines, *Proc IEEE*, 55(1967), 2012–2013.
- [11] Inzoli L.; Rouijaa H.: Aseris: Emcap2000 Esacap software. Applications Handbook and Users Manual, European Aeraunotic Defense and Space, 2001.
- [12] C. R. Paul, *Analysis of Multiconductor Transmission Lines*. New York: Wiley, 1994.